PAPER

NJC
www.rsc.org/njc

Synthesis, spectroscopic properties, and electrochemistry of heteroleptic rare earth double-decker complexes with phthalocyaninato and *meso*-tetrakis (4-chlorophenyl)porphyrinato ligands†

Fanli Lu,[a] Xuan Sun,[a] Renjie Li,[a] Dongbo Liang,[a] Peihua Zhu,[a] Chi-Fung Choi,[b] Dennis K. P. Ng,*[b] Takamitsu Fukuda,[c] Nagao Kobayashi,[c] Ming Bai,[a] Changqin Ma[a] and Jianzhuang Jiang*[a]

[a] *Department of Chemistry, Shandong University, Jinan 250100, China. E-mail: jzjiang@sdu.edu.cn*
[b] *Department of Chemistry, The Chinese University of Hong Kong, Shatin, N.T., Hong Kong, China. E-mail: dkpn@cuhk.edu.hk*
[c] *Department of Chemistry, Graduate School of Science, Tohoku University, Sendai 980-8578, Japan*

Received (in Montpellier, France) 2nd April 2004, Accepted 4th May 2004
First published as an Advance Article on the web 11th August 2004

A series of fourteen heteroleptic (phthalocyaninato)(porphyrinato) rare earth(III) double-decker complexes, [M^{III}(Pc)(TClPP)] [M = Y, La–Lu except Ce and Pm; Pc = phthalocyaninate; TClPP = *meso*-tetrakis (4-chlorophenyl)porphyrinate] has been prepared by base-promoted cyclization of phthalonitrile on the corresponding [M^{III}(TClPP)(acac)] (acac = acetylacetonate) as the template in refluxing *n*-octanol. The yields are highest for the mid-lanthanides, which have the optimum size to balance the stabilization due to π-π interactions and the destabilization due to axial compression of the two π systems. The whole series of double-decker complexes has been characterized by elemental analysis and a wide range of spectroscopic methods. The molecular structure of [Gd^{III}(Pc)(TClPP)] has also been determined. All the electronic absorption bands are dependent on the size of the metal center, suggesting that all the transitions involve molecular orbitals with contributions from both Pc and TClPP ligands. This has been supported by a systematic investigation of the electrochemical properties of the whole series of complexes. All these studies indicate that there are substantial π-π interactions and the hole is mainly localized at the Pc ligand.

Introduction

Sandwich-type phthalocyaninato and/or porphyrinato complexes, in which two or three tetrapyrrole ligands are held by various metal ion(s) in close proximity, have been extensively studied for several decades.[1] Owing to the unique optical, electrical, and magnetic properties, associated with the intriguing intramolecular π-π interactions, these complexes represent an important class of molecular materials for a wide range of applications. While a vast number of homoleptic double- and triple-decker complexes have been reported, the heteroleptic counterparts remain relatively rare.

When different macrocyclic ligands with distinct electronic properties are used, the intramolecular π-π interactions of these complexes can be altered and readily probed by various spectroscopic and electrochemical methods, particularly through a systematic investigation of a whole series of related complexes. We have recently developed several methods to prepare mixed phthalocyaninato, porphyrinato, and/or 2,3-naphthalocyaninato double-deckers, greatly extending this family of compounds.[2] With the exception of the series [M^{III}(Pc)(TPP)] (M = La, Pr, Nd, Eu, Gd, Y, Er, Lu; Pc = phthalocyaninate; TPP = *meso*-tetraphenylporphyrinate) reported by Weiss *et al.*,[3] mixed (phthalocyaninato)(porphyrinato) rare earth double-deckers have only been reported for a few lanthanides, including La,[4] Ce,[5] Eu,[2b,6] Gd,[6a] Tb,[6c] and Y.[2c] No systematic studies for the whole rare earth series have been performed. We describe herein the preparation of a new series of heteroleptic complexes, [M^{III}(Pc)(TClPP)] [M = Y, La–Lu except Ce, Pm; TClPP = *meso*-tetrakis(4-chlorophenyl)-porphyrinate], by the newly developed cyclic tetramerization method.[2b–d] A systematic investigation of the electronic absorption and electrochemical properties of the whole series of complexes has led to a better understanding of the electronic structure and π-π interactions of these novel and rare double-decker complexes.

Results and discussion

Synthesis of [M^{III}(Pc)(TClPP)]

The whole series of the double-decker complexes [M^{III}(Pc)(TClPP)] (M = Y, La–Lu except Ce and Pm; **1**–**14**) was prepared by our recently developed base-promoted cyclization method.[2b–d] The synthesis involves prior generation of the half-sandwich complexes [M^{III}(TClPP)(acac)] from [M(acac)$_3$]·*n*H_2O and H_2(TClPP), followed by treatment with phthalonitrile in the presence of 1,8-diazabicyclo[5.4.0]undec-7-ene (DBU). The yields of these compounds are dependent on

† Electronic supplementary information (ESI) available: reaction yields, analytical and mass spectroscopic data for **1**–**14** (Table S1), plot of wavenumber of the near-IR absorption at 1148–1418 nm *vs.* ionic radius of M^{III} for **1**–**14** (Fig. S1), and plot of the half-wave potentials of **1**–**14** as a function of the ionic radius of M^{III} (Fig. S2). See http://www.rsc.org/suppdata/nj/b4/b404998e/

DOI: 10.1039/b404998e

the size of the metal center. Across the rare earth series, the yield increases from 2% (for M = La) to 36% (for M = Y), then decreases steadily to 11% (for M = Lu) (see Table S1, ESI). It is worth noting that for the bis(porphyrinato) rare earth(III) complexes $[M^{III}(OEP)_2]$ (OEP = octaethylporphyrinate), the yield decreases gradually along the rare earth series,[7] while an opposite trend is observed for the phthalocyaninato analogs $[M^{III}(Pc)_2]$.[8] It seems that for the mixed double-deckers $[M^{III}(Pc)(TClPP)]$, mid-lanthanides have the appropriate size to optimize the separation of the two ligands, leading to a balance between the stabilization due to π-π interactions and the destabilization due to axial compression of the two π systems. As a result, complexes of mid-lanthanides are relatively more stable and can be prepared in higher yield.

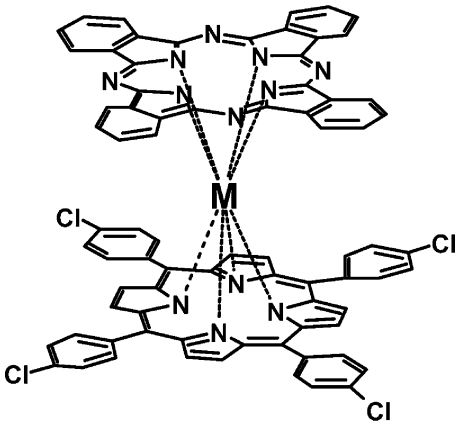

M = Y, La-Lu except Ce and Pm
(1-14)

Spectroscopic characterization

All the new double-deckers **1**–**14** were characterized by elemental analysis (except M = La, Gd) and various spectroscopic methods. The FAB or MALDI-TOF mass spectra of these compounds gave strong signals for the M^+ or MH^+ ions, the isotopic patterns of which were in good agreement with the simulated spectra. This unambiguously confirmed the identity of these compounds. The mass spectral data together with the analytical data are also included in Table S1 of the ESI.

Like other bis(tetrapyrrole) rare earth(III) complexes,[1] the double-deckers $[M^{III}(Pc)(TClPP)]$ (**1**–**14**) contain an unpaired electron in one of the macrocyclic ligands. This was revealed by the EPR spectra of the La (**1**), Y (**9**), and Lu (**14**) analogs. The spectra recorded in CH_2Cl_2 at ambient temperature showed a characteristic signal for organic radicals at $g = 1.997$–1.999 with a peak-to-peak separation of 6.1–11.0 G. Lowering the temperature of **9** to 77 K led to a slight sharpening of signal (peak-to-peak separation = 4.2 G) with the hyperfine structure still remained unresolved. All the remaining double-deckers were ESR-silent under these conditions, due to the interactions between the unpaired electron and the paramagnetic metal center.

Upon addition of hydrazine hydrate, which reduced the double-deckers to the corresponding monoanions $[M^{III}(Pc)(TClPP)]^-$,[9] satisfactory ^1H NMR spectra could be obtained for M = La (**1**), Eu (**5**), Y (**9**), and Lu (**14**). Fig. 1 shows the 2D-COSY spectrum of $[Lu^{III}(Pc)(TClPP)]^-$, which clearly reveals the correlations of all the resonances. The AA′BB′ multiplet at δ 9.00–9.02 is attributed to the Pc α-protons, while the signals for the correlated β-protons are masked by the strong residual $CHCl_3$ signal at δ 8.1. The TClPP β-protons resonate as a sharp singlet at δ 7.90. The four sets of $-C_6H_4Cl$ protons of TClPP, as a result of restricted rotation about the C(*meso*)–C(*ipso*) bond, give two pairs of broad doublets (two of which are overlapped) at δ 6.3–7.5. The spectra for the lanthanum and yttrium analogs are very similar to that of **14**, but the data for the europium counterpart fall into a wider region (δ 5.98–10.73) due to the paramagnetic Eu^{III} center. The NMR data for these compounds together with the assignments are listed in Table 1.

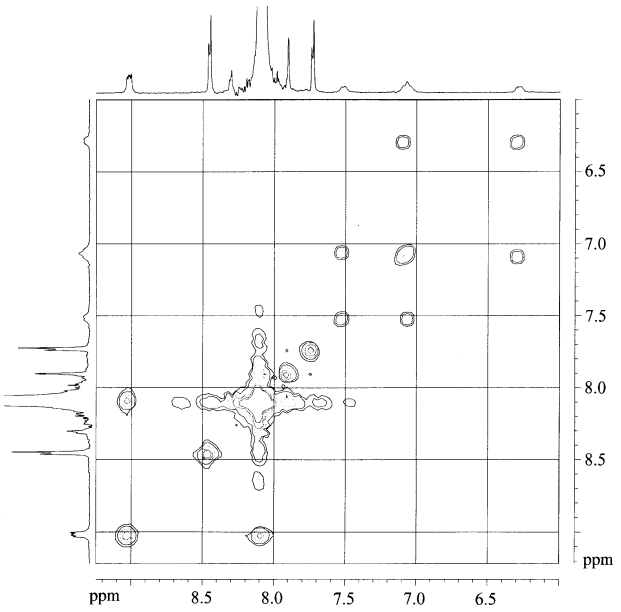

Fig. 1 ^1H–^1H COSY spectrum of $[Lu^{III}(Pc)(TClPP)]$ (**14**) in $CDCl_3$–DMSO-d_6 (1 : 1) in the presence of *ca.* 10% (by volume) hydrazine hydrate.

IR spectroscopy has been proven to be a useful tool for probing the extent of hole delocalization in these sandwich-type complexes.[1,10] Different tetrapyrrole radical anions ($ring^{\bullet -}$) have characteristic IR marker bands. The presence of the $Pc^{\bullet -}$ radical anion in **1**–**14** was revealed by the strong IR marker band at 1311–1320 cm^{-1}.[10,11] The $TClPP^{\bullet -}$ IR marker band at *ca.* 1270–1300 cm^{-1}, however, was not seen for these complexes, showing that the hole is mainly localized in the phthalocyanine ring as a result of its lower first oxidation potential.[12]

Electronic absorption and magnetic circular dichroism (MCD) spectra

The electronic absorption and MCD spectra of this series of double-deckers were measured in $CHCl_3$. The dependence of the spectral features on the metal center is illustrated with the spectra of $[M^{III}(Pc)(TClPP)]$ [M = Sm (**4**), Tb (**7**), Lu (**14**)] as shown in Figs. 2 and 3. All the electronic absorption data are compiled in Table 2. All the absorption spectra (for **1**–**14**) show strong bands at 327–334 and 398–414 nm, which can be attributed to the Soret bands of these complexes having a predominant Pc and TClPP character, respectively.[1,3] The Faraday *A*-term-like dispersion in the MCD spectra for the corresponding signals (Fig. 2) supports this assignment. The absorptions at 467–492 and 923–1089 nm are due to electronic transitions involving the semi-occupied orbital, which has a higher Pc character. An additional characteristic near-IR band for π-radical anions at 1148–1418 nm (with a shoulder at 1587–1697 nm for M = Y, Nd–Lu) can also be observed for the whole series of trivalent rare earth double-deckers $[M^{III}(Pc)(TClPP)]$. As shown in Table 2, the absorption positions of all the absorption bands are sensitive to the ionic radius of the metal center, shifting to the red or blue, depending on the nature of the transition. For instance, when the metal center becomes smaller, the absorption at 923–1089 nm shifts gradually to the red, while the characteristic π-radical

Table 1 ^{1}H NMR data (δ) for the reduced form of the double-deckers [M^{III}(Pc)(TClPP)] (M = La, Eu, Y, Lu) in $CDCl_3$–DMSO-d_6 (1 : 1) with the addition of *ca.* 10% (by volume) hydrazine hydrate[a]

Compound	Pc-H$_\alpha$	Pc-H$_\beta$	TClPP-H$_\beta$	TClPP-H$_{aryl}$
[La(Pc)(TClPP)] (**1**)	9.02–9.04 (m)	–[b]	7.94 (s)	7.51 (br d, J = 8 Hz), 7.24 (br d, J = 8 Hz), 7.13 (br d, J = 8 Hz), 6.75 (br d, J = 8 Hz)
[Eu(Pc)(TClPP)] (**5**)	10.35–10.38 (m)	8.59–8.62 (m)	7.11 (s)	10.73 (br s), 8.68 (br s), 7.30 (br s), 5.98 (br s)
[Y(Pc)(TClPP)] (**9**)	9.01–9.04 (m)	–[b]	7.91 (s)	7.50 (br d, J = 9 Hz), 7.08 (two overlapping br d), 6.37 (br d, J = 9 Hz)
[Lu(Pc)(TClPP)] (**14**)	9.00–9.02 (m)	–[b]	7.90 (s)	7.51 (br d, J = 9 Hz), 7.06 (two overlapping br d), 6.28 (br d, J = 9 Hz)

[a] Multiplicities: s = singlet, d = doublet, m = multiplet, br = broad; coupling constants (J) are reported in Hz. [b] The signals are obscured by the strong residual $CHCl_3$ signal at δ 8.1.

anion band at 1148–1418 nm is blue-shifted in a linear manner (Fig. S1, ESI), so that the energy separation of these two near-IR bands becomes smaller across the series. As shown in Fig. 3, these two near-IR bands coalesce to form a broad signal for the lutetium complex **14**. This result is in line with that observed for [M^{III}(Nc)(OEP)].[2f] Furthermore, a weak absorption in the region of 689–738 nm also appears for this series of double-deckers. This band was neglected previously for analogous complexes.[2b,3,6a] Both the position and intensity of this band are moderately sensitive to the rare earth center. Along with the lanthanide contraction, the band shifts to lower energy (Table 2) and the intensity increases gradually, becoming a distinguishable band for **14** (Fig. 2). This band may be tentatively assigned to one of the Q absorptions for these mixed double-deckers, although the corresponding A terms appear somewhat too small, considering the large angular momentum of the Q band.

Owing to the close proximity of the two conjugated π-systems arranged in a face-to-face manner in **1**–**14**, there are significant interactions between the two macrocyclic ligands. Fig. 4 shows a simplified molecular orbital diagram for this series of complexes constructed from the a_{1u} and e_g orbitals of the two ligands.[13] Due to the ease of oxidation and reduction of Pc compared with TClPP,[12] the a_{1u} orbital of Pc is higher in energy than that of TClPP while the e_g orbitals are lower than those of TClPP. Therefore, both the semi-occupied orbital and the LUMO of [M^{III}(Pc)(TClPP)] are mainly due to the Pc ligand whereas the second HOMO and the second LUMO contain a greater amount of TClPP character. The electronic absorption at 923–1089 nm can thus be attributed to the electronic transition from the semi-occupied orbital to the degenerated LUMO. This is supported by the Faraday A-term-like dispersion observed in the MCD spectra (Fig. 2). The lower energy near-IR absorption at 1148–1418 nm is due to the transition from the second HOMO to the semi-occupied orbital.[14] The changes of the positions of these bands with respect to the metal center are in accord with the extent of π-π interaction, which increases as the size of the metal center decreases. However, the appearance of the lowest energy near-

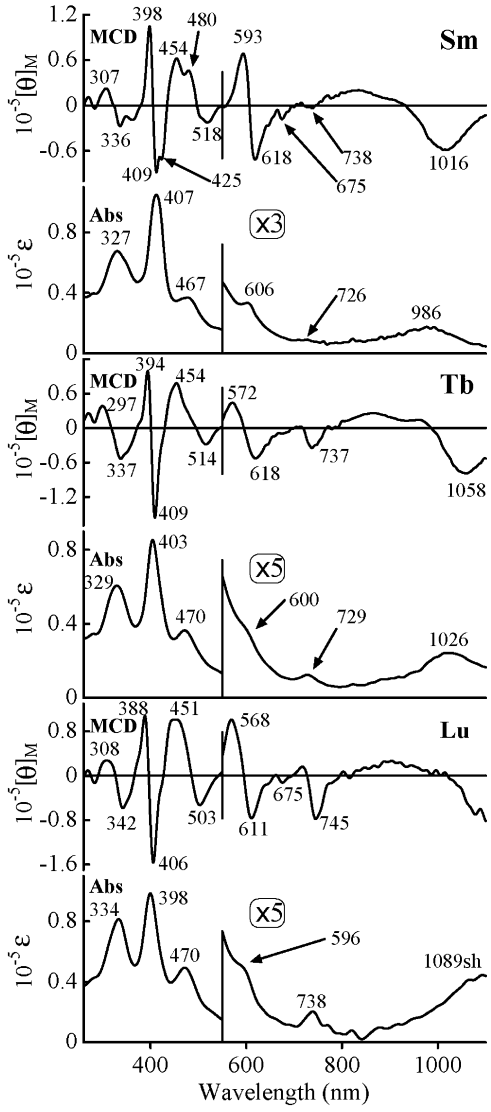

Fig. 2 MCD (upper) and electronic absorption (lower) spectra of [M^{III}(Pc)(TClPP)] [M = Sm (**4**), Tb (**7**), Lu (**14**)] in $CHCl_3$.

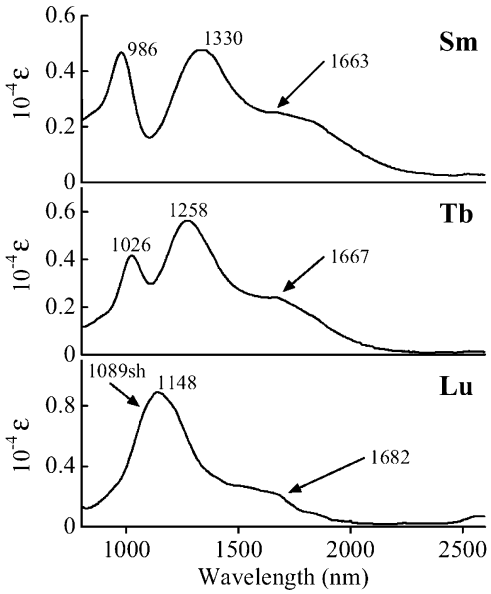

Fig. 3 Near-IR absorption spectra of [M^{III}(Pc)(TClPP)] [M = Sm (**4**), Tb (**7**), Lu (**14**)] in $CHCl_3$.

Table 2 Electronic absorption data for compounds **1**–**14** in $CHCl_3$

Compound	λ_{max}/nm (log ε)						
[La(Pc)(TClPP)] (**1**)	328 (4.77)	414 (5.00)	492 (4.38)	689 (3.47)	923 (3.64)	1418 (3.47)	
[Pr(Pc)(TClPP)] (**2**)	327 (4.87)	411 (5.08)	486 (4.53)	692 (3.62)	954 (3.70)	1376 (3.68)	
[Nd(Pc)(TClPP)] (**3**)	328 (4.79)	411 (4.99)	482 (4.48)	725 (3.37)	969 (3.61)	1377 (3.60)	1693 (3.37)
[Sm(Pc)(TClPP)] (**4**)	327 (4.83)	407 (5.01)	467 (4.57)	726 (3.41)	986 (3.67)	1330 (3.76)	1663 (3.48)
[Eu(Pc)(TClPP)] (**5**)	330 (4.73)	409 (5.13)	473 (4.45)	728 (3.31)	1000 (3.49)	1317 (3.63)	1662 (3.30)
[Gd(Pc)(TClPP)] (**6**)	328 (4.68)	404 (4.85)	472 (4.44)	729 (3.27)	1008 (3.50)	1282 (3.61)	1697 (3.27)
[Tb(Pc)(TClPP)] (**7**)	329 (4.77)	403 (4.93)	470 (4.55)	729 (3.39)	1026 (3.62)	1258 (3.75)	1667 (3.36)
[Dy(Pc)(TClPP)] (**8**)	331 (4.96)	402 (5.10)	470 (4.74)	730 (3.62)	1031 (3.83)	1250 (3.95)	1658 (3.55)
[Y(Pc)(TClPP)] (**9**)	332 (4.92)	401 (5.03)	470 (4.70)	732 (3.55)	1034 (3.79)	1238 (3.91)	1656 (3.49)
[Ho(Pc)(TClPP)] (**10**)	333 (5.02)	402 (5.15)	469 (4.80)	732 (3.68)	1042 (3.89)	1233 (4.00)	1677 (3.47)
[Er(Pc)(TClPP)] (**11**)	333 (4.92)	400 (5.04)	470 (4.70)	734 (3.59)	1054 (3.84)	1228 (3.93)	1637 (3.45)
[Tm(Pc)(TClPP)] (**12**)	334 (4.86)	400 (4.97)	470 (4.64)	734 (3.54)	1069 (3.81)	1211 (3.88)	1631 (3.37)
[Yb(Pc)(TClPP)] (**13**)	334 (4.89)	399 (4.99)	470 (4.68)	736 (3.60)	1070 (3.87)	1161 (3.94)	1623 (3.40)
[Lu(Pc)(TClPP)] (**14**)	334 (4.90)	398 (4.99)	470 (4.69)	738 (3.61)	1089 (3.95)	1148 (3.97)	1587 (3.40)

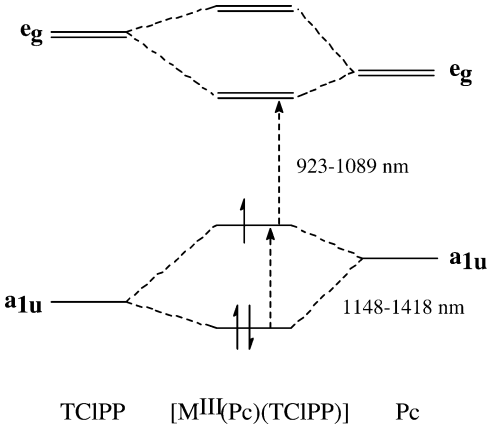

Fig. 4 Simplified molecular orbital diagram for [M^{III}(Pc)(TClPP)].

IR shoulder at 1587–1697 nm is problematic from a band assignment standpoint. The position of this absorption seems to be independent of the size of the metal center. High-level molecular orbital calculations will probably be required to fully investigate the origin of this band.

Molecular structure of [Gd^{III}(Pc)(TClPP)] (6)

The molecular structure of the gadolinium double-decker **6** was also established by X-ray diffraction analysis. This represents one of the few structurally characterized heteroleptic (phthalocyaninato)(porphyrinato) double-decker complexes.[3,4,5a,15] Single crystals suitable for X-ray diffraction analysis were grown by slow diffusion of MeOH into a $CHCl_3$ solution of **6**. The crystal structure was found to contain solvated $CHCl_3$ and H_2O. Fig. 5 shows two perspective views of the molecular structure of **6**. It can be seen that the gadolinium center is octacoordinated by the isoindole and pyrrole nitrogen atoms of the Pc and TClPP rings, respectively, and the coordination polyhedron of the metal is essentially a square antiprism. The average Gd–N(isoindole) and Gd–N(pyrrole) distances are 2.501(9) and 2.452(9) Å, respectively, giving a ring-to-ring separation of 2.824(9) Å. This value is slightly larger than the corresponding value for the oxidized analog $[Gd^{III}(Pc)(TPP)]^+[SbCl_6]^-$ [2.769(5) Å].[3] This can be attributed to the increased ring-to-ring interaction in the oxidized species. The two N_4 mean planes are virtually parallel while the two macrocyclic ligands are significantly domed. The overall structure is similar to those of $[La^{III}(Pc)(TPP)]^3$ and [Ce(Pc)(Por)] [Por = *meso*-tetrakis(4-methoxyphenyl)porphyrinate, *meso*-tetra(4-pyridyl)porphyrinate].[5a,15]

Electrochemical studies

The redox behavior of the heteroleptic double-deckers **1**–**14** was studied by cyclic voltammetry (CV) and differential pulse voltammetry (DPV) in CH_2Cl_2. All these compounds exhibit up to three quasi-reversible one-electron oxidations and three quasi-reversible one-electron reductions. The data are summarized in Table 3. Fig. 6 displays the cyclic and differential pulse voltammograms for [Ho^{III}(Pc)(TClPP)] (**10**), which are typical for the other rare earth counterparts. All these redox processes can be attributed to the successive removal or addition of

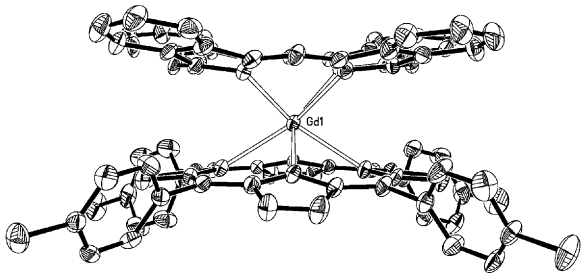

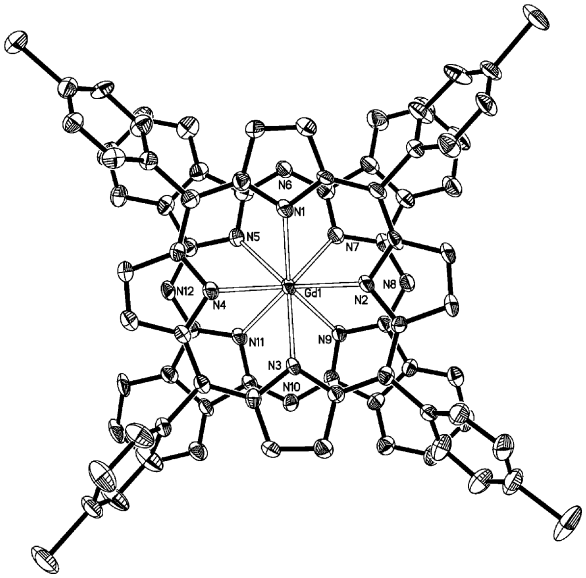

Fig. 5 Molecular structure of [Gd^{III}(Pc)(TClPP)] (**6**) in two perspective views. Hydrogen atoms are omitted for clarity and the ellipsoids are drawn at the 30% probability level.

Table 3 Electrochemical data for compounds **1**–**14**[a]

Compound	O_3	O_2	O_1	R_1	R_2	R_3	$\Delta E_{1/2}$[b]	$\Delta E'_{1/2}$[c]	$\Delta E''_{1/2}$[d]
[La(Pc)(TClPP)] (**1**)		+1.37	+0.80	+0.30	−1.26	−1.74[e]	0.50	0.57	1.56
[Pr(Pc)(TClPP)] (**2**)	+1.59	+1.36	+0.80	+0.27	−1.26	−1.72[e]	0.53	0.56	1.53
[Nd(Pc)(TClPP)] (**3**)	+1.61	+1.41	+0.77	+0.29	−1.25	−1.66	0.48	0.64	1.54
[Sm(Pc)(TClPP)] (**4**)	+1.61[e]	+1.36	+0.70	+0.20	−1.35		0.50	0.66	1.55
[Eu(Pc)(TClPP)] (**5**)	+1.69[e]	+1.39	+0.72	+0.21	−1.28	−1.66[e]	0.51	0.67	1.49
[Gd(Pc)(TClPP)] (**6**)	+1.71	+1.42	+0.73	+0.22	−1.26	−1.66[e]	0.51	0.69	1.48
[Tb(Pc)(TClPP)] (**7**)	+1.71	+1.42	+0.72	+0.21	−1.26	−1.71[e]	0.51	0.70	1.47
[Dy(Pc)(TClPP)] (**8**)	+1.71	+1.41	+0.68	+0.18	−1.28	−1.70	0.50	0.73	1.46
[Y(Pc)(TClPP)] (**9**)	+1.74	+1.41	+0.69	+0.18	−1.28	−1.69[e]	0.51	0.72	1.46
[Ho(Pc)(TClPP)] (**10**)	+1.73	+1.42	+0.69	+0.18	−1.28	−1.71[e]	0.51	0.73	1.46
[Er(Pc)(TClPP)] (**11**)	+1.72	+1.41	+0.65	+0.13	−1.32	−1.72	0.52	0.76	1.45
[Tm(Pc)(TClPP)] (**12**)	+1.75	+1.43	+0.66	+0.15	−1.30	−1.68[e]	0.51	0.77	1.45
[Yb(Pc)(TClPP)] (**13**)	+1.77	+1.43	+0.66	+0.17	−1.28	−1.69[e]	0.49	0.77	1.45
[Lu(Pc)(TClPP)] (**14**)	+1.74	+1.41	+0.63	+0.12	−1.32	−1.69[e]	0.51	0.78	1.44

[a] Recorded with $[Bu_4N][ClO_4]$ as electrolyte in CH_2Cl_2 (0.1 M) at ambient temperature. Potentials were obtained by cyclic voltammetry with a scan rate of 20 mV s^{-1} and are expressed as half-wave potentials ($E_{1/2}$) in V relative to SCE unless otherwise stated. [b] $\Delta E_{1/2} = O_1 - R_1$. [c] $\Delta E'_{1/2} = O_2 - O_1$. [d] $\Delta E''_{1/2} = R_1 - R_2$. [e] By differential pulse voltammetry with a scan rate of 10 mV s^{-1}.

electrons from or to the ligand-based orbitals as the trivalent rare earth center cannot be oxidized or reduced under these conditions. Like many other series of double-deckers,[1] the potentials of some of these processes depend linearly on the ionic radius of the metal center (Fig. S2, ESI). As shown in Table 3 (and Fig. S2 as well), the half-wave potentials of the first oxidation (O_1) and the first reduction (R_1) processes, both of which involve the semi-occupied orbital, decrease slightly as the size of the metal center decreases. In contrast, the potentials of the second (O_2) and third (O_3) oxidation processes, which involve the second HOMO, are shifted in the opposite direction. These results indicate that along with the lanthanide contraction, the energy of the semi-occupied orbital increases gradually while that of the second HOMO decreases. The increase in energy gap between these two orbitals is in accord with the blue-shift of the near IR band at 1148–1418 nm. The potentials for the remaining two reduction processes (R_2 and R_3) are insensitive to the ionic size of the rare earth center, suggesting that the energy level of the LUMO does not change significantly with the metal center. Therefore, the energy separation between the semi-occupied orbital and the LUMO diminishes along with the lanthanide contraction, while that between the second HOMO and the LUMO follows the opposite trend.

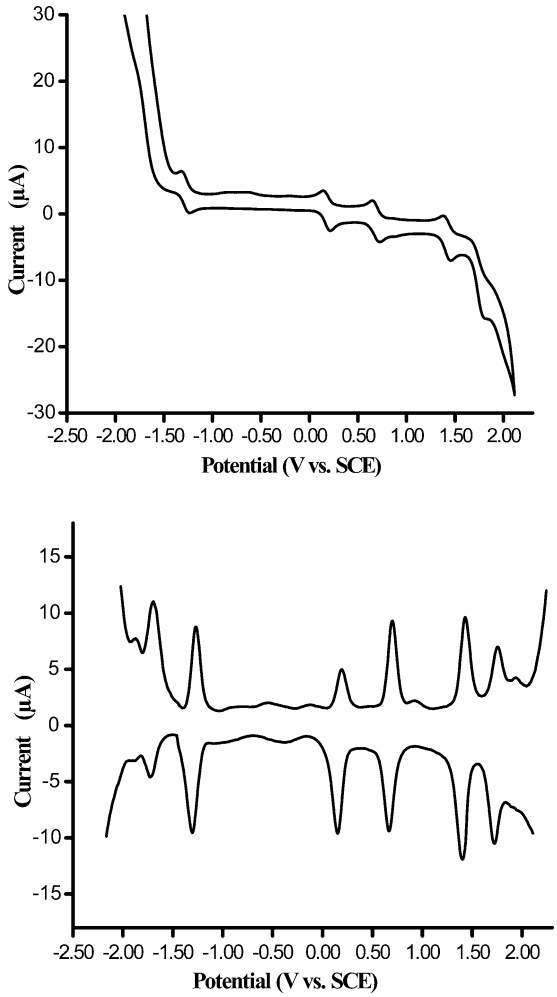

Fig. 6 Cyclic voltammogram (upper) and differential pulse voltammogram (lower) of [Ho^{III}(Pc)(TClPP)] (**10**) in CH_2Cl_2 containing 0.1 M $[Bu_4N][ClO_4]$ at a scan rate of 20 and 10 mV s^{-1}, respectively.

The trends can also be seen from the changes in potential differences across the rare earth series. The potential difference between R_1 and R_2 ($\Delta E''_{1/2}$), which represents the gap between the semi-occupied orbital and the LUMO, decreases gradually from 1.56 V (for M = La) to 1.44 V (for M = Lu), whereas the gap between O_2 and O_1 ($\Delta E'_{1/2}$), which reflects the energy separation between the semi-occupied orbital and second HOMO, increases from 0.57 V (for M = La) to 0.78 V (for M = Lu). These values should be related to the positions of the corresponding electronic transitions (*i.e.*, 923–1089 and 1148–1418 nm, respectively). The opposing trends observed for these two variables in the electrochemical studies is in good agreement with what was observed in the electronic absorption spectroscopic studies (Table 2). The potential difference between O_1 and R_1 ($\Delta E_{1/2}$) for all the double-deckers **1**–**14** spans a relatively narrow range (0.48–0.53 V). The values are slightly larger than those for [M^{III}(Pc)(TPP)] (0.45–0.47 V)[3] and the bis(phthalocyaninato) analogs [M^{III}(Pc^*)$_2$] [Pc* = Pc, 2(3), 9(10),16(17),23(24)-tetra(*tert*-butyl)phthalocyaninate, 2,3, 9, 10, 16, 17, 23, 24-octakis(octyloxy)phthalocyaninate] (0.34–0.46 V).[16]

Conclusion

We have synthesized a series of fourteen heteroleptic rare earth(III) double-deckers [M^{III}(Pc)(TClPP)] (M = Y, La–Lu except Ce and Pm) and characterized them with a wide range of spectroscopic and electrochemical methods. The molecular structure of the gadolinium analog has also been determined. These studies have provided insight about the electronic structure and π-π interactions of these complexes as a function of

the size of the metal center, and revealed that the hole is mainly localized in the phthalocyaninato ligand.

Experimental

General

n-Octanol was distilled from sodium. Hexanes used for chromatography was distilled from anhydrous $CaCl_2$. Column chromatography was carried out on silica gel columns (Merck, Kieselgel 60, 70–230 mesh) with the indicated eluents. Dichloromethane for voltammetric studies was freshly distilled from CaH_2 under nitrogen. The electrolyte $[Bu_4N][ClO_4]$ was recrystallized from tetrahydrofuran. The compounds $[M(acac)_3]\cdot nH_2O$,[17] H_2(TClPP),[18] and Li_2(Pc)[19] were prepared according to literature procedure.

^{1}H NMR spectra were measured on a Bruker DPX 300 spectrometer (300 MHz) in $CDCl_3$–DMSO-d_6 (1 : 1) in the presence of *ca.* 10% (by volume) hydrazine hydrate. Spectra were referenced internally with residual DMSO (δ 2.49). EPR spectra were recorded in CH_2Cl_2 at ambient temperature on a Bruker EMX EPR spectrometer equipped with an ER041 XG microwave bridge (X-band). The field was calibrated using 1,1-diphenyl-2-picrylhydrazyl. Electronic absorption spectra were recorded on a Hitachi U-4100 spectrophotometer. Magnetic circular dichroism (MCD) measurements were made with a JASCO J-725 spectrodichrometer equipped with a JASCO electromagnet that produced magnetic fields (both parallel and antiparallel) of up to 1.09 T. Its magnitude was expressed in terms of molar ellipticity per tesla: $[\theta]_M/10^4$ deg mol^{-1} dm^3 cm^{-1} T^{-1}. IR spectra were recorded as KBr pellets with 2 cm^{-1} resolution using a BIORAD FTS-165 spectrometer. MALDI-TOF mass spectra were taken on a Bruker BIFLEX III ultra-high resolution Fourier transform ion cyclotron resonance (FT-ICR) mass spectrometer with α-cyano-4-hydroxycinnamic acid as a matrix. FAB mass spectra were obtained on a JEOL JMS-HX110 mass spectrometer using 3-nitrobenzyl alcohol as a matrix. Elemental analyses were performed by the Institute of Chemistry, Chinese Academy of Sciences, Beijing.

Electrochemical measurements were carried out with a BAS CV-50W voltammetric analyzer. The cell comprised inlets for a glassy carbon disk working electrode of 2.0 mm in diameter and a silver wire counter electrode. The reference electrode was Ag/Ag^+, which was connected to the solution by a Luggin capillary whose tip was placed close to the working electrode, corrected for junction potentials by being referenced internally to the ferrocenium/ferrocene (Fe^+/Fe) couple ($E_{1/2}[Fe^+/Fe] = 501$ mV *vs.* SCE). Typically, a 0.1 M solution of $[Bu_4N][ClO_4]$ in CH_2Cl_2 containing 0.5 mM of sample was purged with nitrogen for 10 min, then the voltammograms were recorded at ambient temperature. The scan rates were 20 and 10 mV s^{-1} for CV and DPV, respectively.

General procedure for the preparation of 1–14

A mixture of H_2(TClPP) (75 mg, 0.10 mmol) and $[M(acac)_3]\cdot nH_2O$ (0.10 mmol) in *n*-octanol (4 mL) was refluxed under a slow stream of nitrogen. The progress of the reaction was monitored by UV-Vis spectroscopy. After 4–6 h, depending on the metal salt, the transformation to the half-sandwich rare earth complex [M^{III}(TClPP)(acac)] was essentially completed. The mixture was cooled to room temperature, then phthalonitrile (77 mg, 0.60 mmol) and DBU (0.04 mL, 0.26 mmol) were added. The mixture was heated at 120 °C for a further 12 h under nitrogen to give a dark green solution. After cooling, MeOH (60 mL) was added and the precipitate formed was collected by filtration and washed with MeOH. The crude product was purified by chromatography using $CHCl_3$–hexanes (1 : 1) as eluent. A small amount of unreacted H_2(TClPP) was collected first, then the column was further eluted with $CHCl_3$. The green solution obtained, which contained a mixture of [M^{III}H(Pc)(TClPP)] and [M^{III}(Pc)(TClPP)], was exposed to air for several hours to give a brown solution. After removing the solvent *in vacuo*, the residue was chromatographed again under similar conditions and recrystallized from $CHCl_3$ with toluene or MeOH.

Table 4 Crystallographic data for [Gd^{III}(Pc)(TClPP)] (**6**)

	6·$CHCl_3$·H_2O
Formula	$C_{77}H_{43}Cl_7GdN_{12}O$
M_r	1557.63
Crystal system	Monoclinic
Space group	*C*2/*c*
a/Å	38.387 (17)
b/Å	18.997 (8)
c/Å	26.326 (11)
β/°	128.062 (5)
U/Å^3	15 116 (11)
Z	8
μ/mm^{-1}	1.176
Reflections collected	39 147
Independent reflections	13 321
R_{int}	0.0898
*R*1 [$I > 2\sigma(I)$]	0.0802
*wR*2 [$I > 2\sigma(I)$]	0.2340

X-Ray crystallographic analysis of 6

Crystal data and details of data collection and structure refinement are given in Table 4. Data were collected on a Bruker SMART CCD diffractometer with an $Mo_{K\alpha}$ sealed tube ($\lambda = 0.71073$ Å) at 293 K, using a ω scan mode with an increment of 0.3°. Preliminary unit cell parameters were obtained from 45 frames. Final unit cell parameters were obtained by global refinements of reflections obtained from integration of all the frame data. The collected frames were integrated using the preliminary cell-orientation matrix. SMART software was used for collecting frames of data, indexing reflections, and determination of lattice constants; SAINT-PLUS for integration of intensity of reflections and scaling;[20] SADABS for absorption correction;[21] and SHELXTL for space group and structure determination, refinements, graphics, and structure reporting.[22] ‡

Acknowledgements

We thank Prof. Hung-Kay Lee for recording the EPR spectra and Hoi-Shan Chan for refining the structure of **6**. Financial support from the National Natural Science Foundation of China (Grant No. 20171028, 20325105), National Ministry of Science and Technology of China (Grant No. 2001CB6105-04), National Ministry of Education of China, Shandong University, The Chinese University of Hong Kong, and Ministry of Education, Culture, Sports, Science, and Technology of Japan (Grant-in-Aid for the COE project "Giant Molecules and Complex Systems" 2003) is gratefully acknowledged.

References

1 (*a*) D. K. P. Ng and J. Jiang, *Chem. Soc. Rev.*, 1997, **26**, 433; (*b*) J. W. Buchler and D. K. P. Ng, in *The Porphyrin Handbook*, eds. K. M. Kadish, K. M. Smith and R. Guilard, Academic Press, San Diego, 2000, vol. **3**, pp. 245–294; (*c*) J. Jiang, K. Kasuga and D. P. Arnold, in *Supramolecular Photo-sensitive and Electro-active*

‡ CCDC reference number 226014. See http://www.rsc.org/suppdata/nj/b4/b404998e/ for crystallographic data in .cif or other electronic format.

Materials, ed. H. S. Nalwa, Academic Press, New York, 2001, pp. 113–210; (*d*) J. Jiang, W. Liu and D. P. Arnold, *J. Porphyrins Phthalocyanines*, 2003, **7**, 459.
2 See, for example: (*a*) J. Jiang, W. Liu, W.-F. Law, J. Lin and D. K. P. Ng, *Inorg. Chim. Acta*, 1998, **268**, 141; (*b*) J. Jiang, M. T. M. Choi, W.-F. Law, J. Chen and D. K. P. Ng, *Polyhedron*, 1998, **17**, 3903; (*c*) J. Jiang, J. Xie, M. T. M. Choi, Y. Yan, S. Sun and D. K. P. Ng, *J. Porphyrins Phthalocyanines*, 1999, **3**, 322; (*d*) J. Jiang, D. Du, M. T. M. Choi, J. Xie and D. K. P. Ng, *Chem. Lett*., 1999, 261; (*e*) J. Jiang, W. Liu, K.-L. Cheng, K.-W. Poon and D. K. P. Ng, *Eur. J. Inorg. Chem*., 2001, 413; (*f*) J. Jiang, Y. Bian, F. Furuya, W. Liu, M. T. M. Choi, N. Kobayashi, H.-W. Li, Q. Yang, T. C. W. Mak and D. K. P. Ng, *Chem. Eur. J*., 2001, **7**, 5059; (*g*) Y. Bian, R. Wang, J. Jiang, C.-H. Lee, J. Wang and D. K. P. Ng, *Chem. Commun*., 2003, 1194.
3 D. Chabach, M. Tahiri, A. De Cian, J. Fischer, R. Weiss and M. El. Malouli Bibout, *J. Am. Chem. Soc*., 1995, **117**, 8548.
4 M. Tahiri, D. Chabach, M. El. Malouli-Bibout, A. De Cian, J. Fischer and R. Weiss, *Ann. Chim*., 1995, **20**, 81.
5 (*a*) M. Lachkar, A. De Cian, J. Fischer and R. Weiss, *New J. Chem*., 1988, **12**, 729; (*b*) T.-H. Tran-Thi, T. Fournier, A. De Cian, D. Chabach, R. Weiss, D. Houde, C. Pépin and L. Dao, *Chem. Phys. Lett*., 1993, **213**, 139; (*c*) T.-H. Tran-Thi, T. A. Mattioli, D. Chabach, A. De Cian and R. Weiss, *J. Phys. Chem*., 1994, **98**, 8279.
6 (*a*) J. Jiang, T. C. W. Mak and D. K. P. Ng, *Chem. Ber*., 1996, **129**, 933; (*b*) T. Gross, F. Chevalier and J. S. Lindsey, *Inorg. Chem*., 2001, **40**, 4762; (*c*) N. Pan, J. Jiang, X. Cui and D. P. Arnold, *J. Porphyrins Phthalocyanines*, 2002, **6**, 347.
7 J. W. Buchler, J. Hüttermann and J. Löffler, *Bull. Chem. Soc. Jpn*., 1988, **61**, 71.
8 C. Clarisse and M. T. Riou, *Inorg. Chim. Acta*, 1987, **130**, 139.
9 (*a*) A. Pondaven, Y. Cozien and M. L'Her, *New J. Chem*., 1992, **16**, 711; (*b*) F. Guyon, A. Pondaven, P. Guenot and M. L'Her, *Inorg. Chem*., 1994, **33**, 4787.
10 (*a*) J. Jiang, D. P. Arnold and H. Yu, *Polyhedron*, 1999, **18**, 2129; (*b*) X. Sun, M. Bao, N. Pan, X. Cui, D. P. Arnold and J. Jiang, *Aust. J. Chem*., 2002, **55**, 587; (*c*) F. Lu, M. Bao, C. Ma, X. Zhang, D. P. Arnold and J. Jiang, *Spectrochim. Acta, Part A*, 2003, **59**, 3273; (*d*) M. Bao, N. Pan, C. Ma, D. P. Arnold and J. Jiang, *Vib. Spectrosc*., 2003, **32**, 175.
11 K. M. Kadish, G. Moninot, Y. Hu, D. Dubois, A. Ibnlfassi, J.-M. Barbe and R. Guilard, *J. Am. Chem. Soc*., 1993, **115**, 8153.
12 (*a*) G. Hariprasad, S. Dahal and B. G. Maiya, *J. Chem. Soc., Dalton Trans*., 1996, 3429; (*b*) M. L'Her and A. Pondaven, in *The Porphyrin Handbook*, eds. K. M. Kadish, K. M. Smith and R. Guilard, Academic Press, San Diego, 2003, vol. **16**, pp. 117–169.
13 (*a*) E. Orti, J. L. Bredas and C. Clarisse, *J. Chem. Phys*., 1990, **92**, 1228; (*b*) R. Rousseau, R. Aroca and M. L. Rodriguez-Mendez, *J. Mol. Struct*., 1995, **356**, 49.
14 According to the "supermolecular" MO model, this characteristic absorption can be attributed to the electronic transition from the second-highest-filled supermolecular bonding orbital to the half-filled supermolecular antibonding orbital. See: (*a*) J. K. Duchowski and D. F. Bocian, *J. Am. Chem. Soc*., 1990, **112**, 3312; (*b*) O. Bilsel, J. Rodriguez, S. N. Milam, P. A. Gorlin, G. S. Girolami, K. S. Suslick and D. Holten, *J. Am. Chem. Soc*., 1992, **114**, 6528.
15 Y. Bian, J. Jiang, Y. Tao, M. T. M. Choi, R. Li, A. C. H. Ng, P. Zhu, N. Pan, X. Sun, D. P. Arnold, Z.-Y. Zhou, H.-W. Li, T. C. W. Mak and D. K. P. Ng, *J. Am. Chem. Soc*., 2003, **125**, 12 257.
16 P. Zhu, F. Lu, N. Pan, D. P. Arnold, S. Zhang and J. Jiang, *Eur. J. Inorg. Chem*., 2003, 510.
17 J. G. Stites, C. N. McCarty and L. L. Quill, *J. Am. Chem. Soc*., 1948, **70**, 3142.
18 G. H. Barnett, M. F. Hudson and K. M. Smith, *J. Chem. Soc., Perkin Trans. 1*, 1975, 1401.
19 P. A. Barrett, D. A. Frye and R. P. Linstead, *J. Chem. Soc*., 1938, 1157.
20 *SMART 5.0 and SAINT 4.0 for Windows NT*, Area Detector Control and Integration Software, Bruker Analytical X-Ray Systems, Madison, WI, 1998.
21 G. M. Sheldrick, *SADABS: Program for Empirical Absorption Correction of Area Detector Data*, University of Göttingen, Germany, 1996.
22 G. M. Sheldrick, SHELXTL 5.1 for Windows NT: Structure Determination Software Programs, Bruker Analytical X-Ray Systems, Madison, WI, 1997.